

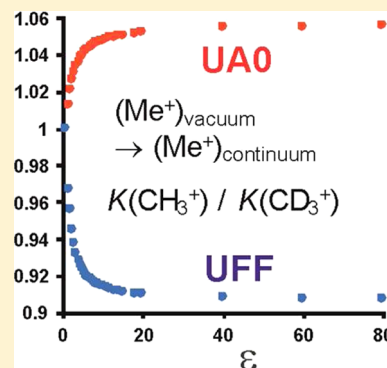
Solvent Effects on Isotope Effects: Methyl Cation as a Model System

Philippe B. Wilson, Paul J. Weaver, Ian R. Greig, and Ian H. Williams*

Department of Chemistry, University of Bath, Bath BA2 7AY, United Kingdom

S Supporting Information

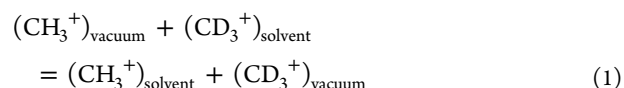
ABSTRACT: The isotopic sensitivity (CH_3^+ vs CD_3^+) of the equilibrium between the methyl cation in vacuum and in solution has been investigated. Two alternative options for describing the shape of the solute cavity within the widely used polarized continuum model for implicit solvation were compared; the UFF and UA0 methods give equilibrium isotope effects (EIEs) that vary as a function of the dielectric constant in opposite directions. The same isotope effect was also obtained as the average over 40 structures from a hybrid quantum mechanical/molecular mechanical molecular dynamics simulation for the methyl cation explicitly solvated by many water molecules; the inverse value of the EIE agrees with UFF but not UA0. The opposing trends may be satisfactorily explained in terms of the different degrees of exposure of the atomic charges to the dielectric continuum in cavities of different shapes.



■ INTRODUCTION

Isotope effects on rates and equilibria are very important experimental probes in mechanistic investigations.¹ Solvent effects on reaction mechanisms are well-known,² but solvent effects on isotope effects are rather less well understood. Changing the solvent can alter a kinetic isotope (KIE) indirectly by affecting the transition-state (TS) structure.³ For example, in Menshutkin reactions, a more polar solvent may stabilize the ionic products more effectively and give an “earlier” TS, as accounted for by the Hammond postulate, which in turn may give rise to a less inverse secondary α -deuterium ($2^\circ \alpha$ -D) KIE;^{4,5} again, as the solvent becomes more ionizing and less nucleophilic in solvolyses of 2-propyl- β -naphthalenesulfonate, the rate-determining step shifts from substitution to ionization and then to dissociation within an $\text{S}_{\text{N}}2$ – $\text{S}_{\text{N}}1$ mechanistic spectrum.⁶ Changing the solvent can also alter a KIE indirectly by affecting the mechanism; in Shiner’s generalized model for solvolytic substitution at saturated carbon, changing the solvent may alter the identity of the rate-determining step, as indicated by the magnitude and direction of the measured $2^\circ \alpha$ -D KIE.⁷ Bentley has questioned several assumptions within Shiner’s model, including that single-step α -D KIEs for non- $\text{S}_{\text{N}}2$ mechanisms are independent of solvent,⁸ and has suggested that solvolyses of secondary alkyl sulfonates can be rationalized by a model combining heterolysis with nucleophilic solvent participation.⁹ Changing the solvent may also influence a KIE by affecting isotopically sensitive vibrational frequencies directly, regardless of the TS structure or the identity of a rate-determining step. This was recognized by Keller and Yankwich, who investigated simple models that might allow medium effects on heavy-atom KIEs to be estimated,^{10–12} but their work seems to have been largely overlooked along with the wider issue.

As part of our long-standing program of computational studies of KIEs for aliphatic nucleophilic substitution^{13–20} and, in particular, enzyme-catalyzed methyl transfer,^{21–24} we are now investigating medium effects on KIEs for $\text{S}_{\text{N}}2$ methyl transfer. In a formal sense, the methyl group transfers between a nucleophile and a nucleofuge as “ CH_3^+ ”, although the size of the charge on the methyl group in the $\text{S}_{\text{N}}2$ TS may be much less than +1, depending on the extents of bond making and breaking. Of course, nucleophilic substitution reactions of methyl substrates in solution never go by the $\text{S}_{\text{N}}1$ mechanism involving the methyl cation as a discrete intermediate. Nonetheless, in order to understand what actually happens in experimentally observed reactions, it is of interest to calibrate experimental isotope effects against those computed for model processes involving the bare methyl cation. Here, we report results from two very different types of calculation of medium effects upon equilibrium isotope effects (EIEs) for the methyl cation (eq 1). First, we contrast the opposite trends in EIEs for transfer of the methyl cation from vacuum into implicit solvent, described using either the UFF or the UA0 cavity method within the polarized continuum model (PCM). Second, we employ a hybrid quantum mechanical/molecular mechanical (QM/MM) method for explicit solvation of the methyl cation by water in order to determine which version of the implicit solvation model is likely to be correct.



Special Issue: William L. Jorgensen Festschrift

Received: May 30, 2014

Revised: July 8, 2014

Published: July 10, 2014

METHODS

Geometry optimization and harmonic frequency calculations were performed initially (2007) with Gaussian03 (revision B.04)²⁵ and subsequently (2014) with Gaussian09 (revision A.02).²⁶ The IEFPCM solvation model was used with the B3LYP density functional and the aug-cc-PVDZ basis set; this combination of method and basis set had been shown to give the best agreement between calculation and experiment for KIEs involving six isotope substitutions in the reaction of a cyanide anion with chloroethane.²⁷ The Gaussian03-default United-Atom Topological Model (UA0) solute cavity was used with both versions of Gaussian, both with its default radius (2.525 Å centered on carbon and defining a sphere including the three hydrogen atoms) and with user-specified radii; with this cavity model, hydrogen atoms are enclosed within the sphere of the heavy atom to which they are bonded, such that the methyl cation is always spherical in shape. The Gaussian09-default United Force Field (UFF) solute cavity was also used with both versions of Gaussian, both with its default radii for carbon and hydrogen and with user-specified radii; this cavity model gives each hydrogen atom its own radius, such that the methyl cation generally has the familiar shape of a CPK space-filling model. All other solvent cavity parameters were set to the default values for water, but the value of the dielectric constant was varied. These implicit solvent calculations were repeated using the AM1 semiempirical method in Gaussian09 to facilitate comparison with the explicit solvent QM/MM calculations.

The D_3 isotopic partition function ratios f_e (eq 2) for the AM1 methyl cation in vacuum ($\epsilon = 1$) and in a continuum solvent ($\epsilon = 1.5$ –80) were calculated using $3N - 6$ pure vibrational degrees of freedom, as previously described;^{28,29} the six translational and rotational degrees of freedom of the isotopologues were replaced by the vibrational product according to the Teller–Redlich product rule, analogously to the Bigeleisen equation. The prime (') in eq 2 denotes the heavy isotopologue CD_3 (as opposed to the unprimed CH_3), N is the number of atoms, ν is a vibrational frequency, and $u = h\nu/k_B T$, where h , k_B , and T are the Planck and Boltzmann constants and the absolute temperature. The term involving atomic masses m differs from unity by virtue of the isotopically substituted atoms only and vanishes from the EIE because it is identical in both top and bottom of the quotient in eq 5.

$$f_e = \prod_i^{3N-6} \left[\frac{\nu'_i \sinh(u_i/2)}{\nu_i \sinh(u'_i/2)} \right] \left[\prod_j^N \frac{m_j}{m'_j} \right]^{3/2} \quad (2)$$

QM/MM molecular dynamics, energy minimization, and Hessian evaluation calculations were performed by means of the fDynamo program.³⁰ The AM1-optimized methyl cation was placed in the center of a pre-equilibrated 40 Å cube of ~2000 TIP3P water molecules, and a switched cutoff radius of 15.5 Å was employed. A 200 ps molecular dynamics simulation with periodic boundary conditions was performed at 300 K using the NVT ensemble with a time step of 1 fs. A snapshot structure was taken every 5 ps and used as the starting point for a QM/MM energy minimization of an AM1 core, composed of the methyl cation and all water molecules within 4 Å, within a frozen environment of all of the remaining TIP3P waters.

A “full subset” Hessian was evaluated for the QM core of each structure; these ranged in size from 120×120 to 210×210 , depending on how many water molecules were included.

These Hessians were then subjected to the “cut-off” procedure previously described¹⁸ in order to exclude all elements involving atoms of water and to reduce the dimension of the Hessian to 12×12 (corresponding to the methyl atoms only). The D_3 isotopic partition function ratio f_s (eq 3) was calculated using all $3N_s$ vibrational degrees of freedom, as previously described,¹⁸ where N_s is either the total number of atoms ($40 \leq N_s \leq 70$) including water molecules in the first solvation shell (full subset) or simply $N_s = 4$ (cutoff). Note that there is no separation of vibrational from translational and rotational degrees of freedom, and it is neither correct nor necessary to use the Bigeleisen formalism.¹⁸ The average isotopic partition function ratio $\langle f_s \rangle$ was obtained as the arithmetic mean of the values for all of the individual locally relaxed structures (eq 4).

$$f_s = \prod_i^{3N_s} \left[\frac{\nu'_i \sinh(u_i/2)}{\nu_i \sinh(u'_i/2)} \right] \left[\prod_j^N \frac{m_j}{m'_j} \right]^{3/2} \quad (3)$$

$$\langle f_s \rangle = \frac{1}{40} \sum_j^{40} (f_s)_j \quad (4)$$

The EIE $K(CH_3)/K(CD_3)$ for transfer of the methyl cation from vacuum to solvent is equivalent to the equilibrium constant for the formal equilibrium shown in eq 1, whose value is obtained from either eq 5 or 6; the isotopic partition function ratios and the EIE were evaluated at 298 K.

implicit solvation:

$$EIE = \frac{f_1}{f_e} \quad (5)$$

explicit solvation:

$$EIE = \frac{f_1}{\langle f_s \rangle} \quad (6)$$

Valence force constants were obtained from Hessians in Cartesian coordinates by means of standard methods using our Camvib program.²⁸

RESULTS AND DISCUSSION

Implicit Solvation. Figure 1 shows the results of the B3LYP/aug-cc-PVDZ EIE calculations comparing the two alternative methods for defining the solute cavity within the PCM method. The CH bond length of the trigonal planar methyl cation was reoptimized for each value of the dielectric constant, and all of the parameters in eq 2 for the isotopic partition function ratio were re-evaluated; the default atom radii were used for both the UA0 and UFF methods. Several observations are noteworthy.

(i) The UA0 (red) and UFF (blue) EIEs tend toward completely different limiting values as the dielectric constant increases to a value corresponding to water as the solvent (Figure 1a). The UA0 method predicts increasingly normal EIEs, tending toward ~1.06 as $\epsilon \rightarrow \infty$, implying that the methyl cation is “looser” in the PCM solvent than that in vacuum. The UFF method predicts increasingly inverse EIEs, tending toward ~0.90 as $\epsilon \rightarrow \infty$, implying that the methyl cation is “tighter” in the PCM solvent than that in vacuum. Both methods cannot be correct!

(ii) Identical results are obtained using either Gaussian03 or Gaussian09. It may be noted that, whereas UA0 was the default

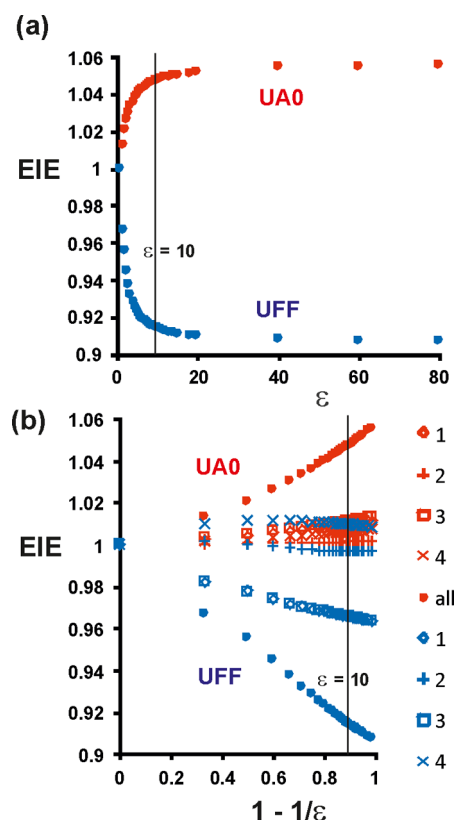


Figure 1. Calculated EIEs $K(\text{CH}_3)/K(\text{CD}_3)$ at 298 K for transfer of a methyl cation from vacuum to continuum solvent using the PCM/B3LYP/avg-cc-PVDZ method, with either the UA0 (red) or UFF (blue) cavities with default atom radii, as a function of (a) dielectric constant ϵ and (b) $1 - 1/\epsilon$. Solid circles denote full EIEs, and other symbols denote normal-mode factors: \diamond , CH stretch (ν_1 , a_1'); \square , degenerate CH stretches (ν_3 , e'); +, out-of-plane bend (ν_2 , a_2''); \times , degenerate in-plane bends (ν_4 , e').

method in the earlier program, UFF is the default in the later program. Differences in other molecular properties calculated with continuum solvation methods in the two versions have been noted by other workers.³¹

(iii) The qualitative shape of each curve is the same as that for the $(1 - 1/\epsilon)$ factor in the Born model for the electrostatic contribution of the free energy of solvation of a point charge within a spherical cavity.³² The solvation energies relative to vacuum are, of course, all negative quantities for both methods, and their magnitudes change with respect to the dielectric constant in the same way as the EIEs; the UFF solvation energy for $\epsilon = 80$ is, at -304 kJ mol^{-1} , more stabilizing by 56 kJ mol^{-1} than the UA0 value. EIEs calculated by means of eqs 2 and 5 may be factorized into normal-mode contributions, which are shown in Figure 1b as plots versus $(1 - 1/\epsilon)$; the overall EIEs for UA0 (solid red circles) and UFF (solid blue circles) give nonlinear plots as the PCM method is not as simple as the Born model.

(iv) In each case, the contribution (114%) of the CH stretching modes (ν_1 , open diamonds, and the degenerate ν_3 , open squares, Figure 1b) to the EIE is more important than that (−14%) of the bending modes (ν_2 , “+”, and the degenerate ν_4 , “ \times ”, Figure 1b). In particular, the out-of-plane bending mode makes only a very small contribution to the dielectric sensitivity of the EIEs for both UA0 and UFF cavity models.

The EIEs are dominated by zero-point energy differences (see the Supporting Information for further details).

(v) About 80% of the change in the EIE from unity occurs within the range of $1 \leq \epsilon \leq 10$ for both methods. This fact has possible implications for computational modeling of isotope effects in enzyme-catalyzed methyl transfer reactions and perhaps enzyme-catalyzed reactions in general because local values of the dielectric constant in proteins and enzyme active sites generally span more or less the same range.³³ In some circumstances, it is conceivable that a reaction involving charge redistribution, separation, or neutralization within an enzyme active site could manifest variations in KIEs, as between a wild-type and a mutant form of the enzyme, that originate from changes in the local dielectric response within the inhomogeneous protein environment. This could have important implications for the interpretation of experimental KIEs in mechanistic enzymology.

(vi) The AM1 semiempirical method shows exactly the same qualitative behavior but with somewhat smaller magnitudes for the EIEs, which tend toward limits of ~ 1.03 for UA0 and ~ 0.97 as $\epsilon \rightarrow \infty$.

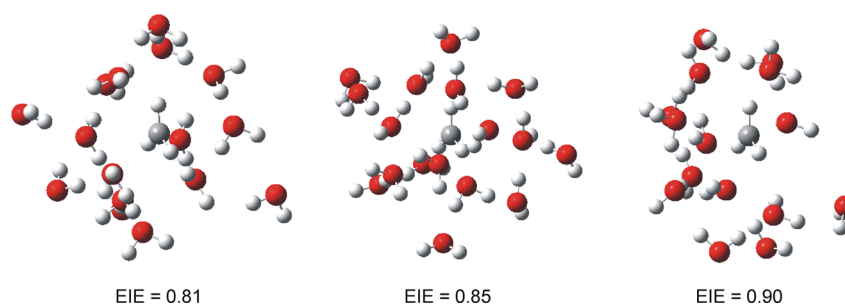
Explicit Solvation. Table 1 contains AM1/TIP3P isotopic partition function ratios f_s calculated by means of eq 3 for perdeuterium substitution in the methyl cation in water, along with the AM1 ratio f_1 in vacuum. The CD_3 EIE for transfer of methyl cation from vacuum to explicit water is obtained by dividing f_1 by the mean of f_s , which yields a value of 0.85 ± 0.02 . The inverse EIE indicates that the H/D atoms in the methyl cation experience, on average, a “tighter” bonding environment in water than that in vacuum. The valence force constants for CH/D bond stretching are given in Table 1 to illustrate not only that, on average, these bonds are significantly stiffer in water than in vacuum but also that there is considerable asymmetry within each locally relaxed structure in water, reflecting the inhomogeneity of solvation within each of the 40 instantaneous snapshots taken from the MD simulation. The locally relaxed structures contain between 12 and 22 water molecules within their QM cores, none of which collapsed to protonated methanol during energy minimization.

In general, isotopic partition function ratios may be averaged over structures containing different numbers of atoms because each pair of isotopologues contains the same number,^{19,20} as happens for the full subset EIEs reported in Table 1. However, the cutoff EIEs for individual structures are almost identical, and their average value is the same as that for the full subset. Each cutoff value of f_s is obtained by means of eq 3, which involves a product function over all 12 (internal) vibrational and (external) librational modes of the methyl cation within its solvent environment. The variation seen in the isotopic partition function ratios reflects variation in the curvature of the potential energy hypersurface in the immediate vicinity of the methyl group arising from structural variation in the solvation shell and cybotactic region of the aqueous solvent. It is important to note that the frozen MM environment exerts its influence on the full subset Hessian for the QM core by virtue of the QM/MM interaction term, and evidently, this influence is manifest even in the elements of the cutoff Hessian.

Figure 2 shows energy-minimized structures for the QM cores of 3 of the 40 different solvent configurations around the methyl cation; these are selected because they give rise to the most and the least inverse EIEs as well as to an EIE very close to the overall mean value. There is no obvious way to tell which is which by simple visual inspection of the structures.

Table 1. AM1/TIP3P Isotopic Partition Function Ratios and D₃ EIEs (298 K) for Transfer of a Methyl Cation from Vacuum to Explicit Water and Valence Force Constants for CH Bond Stretching

structure	QM waters	f_s cutoff	EIE cutoff	EIE full subset	$F_{CH}/aJ \text{ \AA}^{-2}$		
vacuum	0	15172 ^a	1	1	5.134	5.134	5.134
1	13	17512	0.866	0.867	5.280	5.181	5.283
2	15	17038	0.890	0.892	5.213	5.214	5.196
3	17	18323	0.828	0.829	5.279	5.285	5.201
4	15	18148	0.836	0.837	5.153	5.289	5.297
5	16	17673	0.858	0.860	5.253	5.268	5.199
6	16	18776	0.808	0.810	5.275	5.247	5.264
7	16	17819	0.851	0.852	5.256	5.320	5.339
8	13	17532	0.865	0.866	5.279	5.179	5.285
9	15	17914	0.847	0.848	5.334	5.281	5.212
10	12	17528	0.866	0.866	5.203	5.300	5.265
11	14	17776	0.854	0.855	5.263	5.132	5.281
12	13	18374	0.826	0.827	5.161	5.308	5.284
13	13	17613	0.861	0.863	5.228	5.272	5.270
14	16	17115	0.886	0.888	5.186	5.235	5.245
15	17	17641	0.860	0.861	5.246	5.318	5.253
16	18	18414	0.824	0.825	5.265	5.234	5.332
17	18	17983	0.844	0.845	5.289	5.272	5.307
18	15	18180	0.835	0.836	5.292	5.204	5.327
19	13	17760	0.854	0.855	5.319	5.273	5.214
20	14	18455	0.822	0.823	5.356	5.177	5.379
21	13	17674	0.858	0.860	5.299	5.164	5.333
22	15	17950	0.845	0.846	5.240	5.239	5.305
23	15	17561	0.864	0.865	5.187	5.300	5.251
24	17	17874	0.849	0.850	5.222	5.288	5.310
25	15	16834	0.901	0.902	5.111	5.178	5.280
26	22	17780	0.853	0.855	5.333	5.284	5.208
27	18	17236	0.880	0.882	5.253	5.226	5.236
28	17	17675	0.858	0.859	5.171	5.317	5.287
29	16	17718	0.856	0.858	5.297	5.337	5.085
30	18	17741	0.855	0.857	5.245	5.281	5.264
31	18	17644	0.860	0.861	5.306	5.315	5.173
32	17	17181	0.883	0.885	5.228	5.224	5.213
33	16	17782	0.853	0.854	5.310	5.082	5.305
34	14	18056	0.840	0.841	5.267	5.319	5.291
35	17	17497	0.867	0.868	5.273	5.233	5.358
36	15	18457	0.822	0.823	5.407	5.245	5.335
37	12	18365	0.826	0.827	5.225	5.145	5.247
38	19	17855	0.850	0.851	5.269	5.168	5.265
39	14	17752	0.855	0.856	5.288	5.268	5.308
40	14	17503	0.867	0.868	5.169	5.280	5.347
mean		17793	0.853	0.854	5.258		
$1\sigma^b$		± 418	± 0.020	± 0.020	± 0.059		

^a f_s ^b 1σ is a single standard deviation.**Figure 2.** AM1/TIP3P energy-minimized QM cores of three structures giving rise to very different EIEs $K(\text{CH}_3)/K(\text{CD}_3)$ for transfer of the methyl cation from vacuum into water.

The purpose of the explicit solvent QM/MM calculations was to provide an independent determination of the EIE in order to discriminate between the opposite trends of the UA0 and UFF cavity methods within the implicit solvent treatment. The current AM1/TIP3P results are unlikely to be definitive quantitatively because of both the limitations of this choice of QM/MM method and the small number of structures sampled. Nonetheless, in a qualitative sense, the average EIE = 0.85 obtained for explicit water is in accord with the prediction of the UFF method but is very clearly incompatible with the UA0 result.

Why Do UFF and UA0 Behave so Differently? Figure 3a shows the variation in the PCM/B3LYP/aug-cc-PVDZ

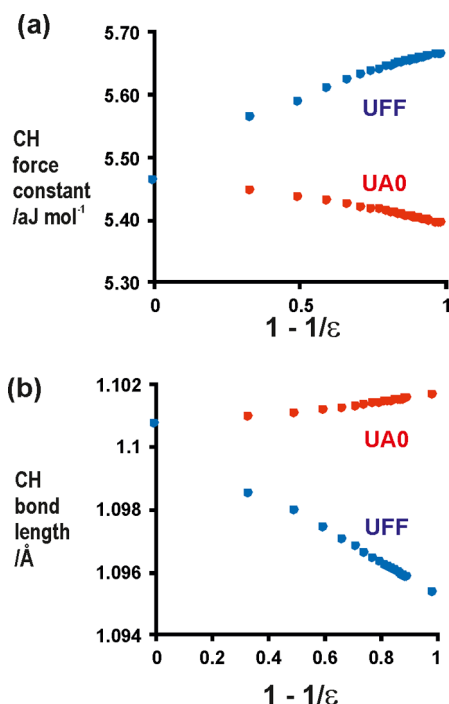


Figure 3. (a) PCM/B3LYP/aug-cc-PVDZ CH bond stretching force constants and (b) optimized CH bond lengths for methyl cation in continuum solvent as a function of $1 - 1/\epsilon$.

calculated valence force constants for CH bond stretching in the methyl cation as a function of $(1 - 1/\epsilon)$. The two cavity models clearly show opposite trends that correspond to the behavior of the EIEs; increasing the polarity of the continuum solvent leads to looser force constants with UA0 (and hence larger normal EIEs) but to stiffer force constants with UFF (and hence larger inverse EIEs). Figure 3b shows the accompanying changes in optimized CH bond lengths, getting slightly longer in UA0 (over a narrow range) with increasing dielectric constant but significantly shorter in UFF (over a wide range).

The electrostatic potential fitted (ESP) charge on the carbon atom is plotted against the CH bond length in Figure 4a; the UA0 and UFF data points all lie on an excellent linear correlation. The graph of solvation energy against bond length, Figure 4b, highlights the difference between the two methods. UFF gives a very good linear correlation, showing increasing stabilization of the methyl cation with decreasing CH bond length. On the other hand, the UA0 solvation energy increases quadratically with increasing bond length. It is not possible to extend the CH bond very far with the UA0 method as the H

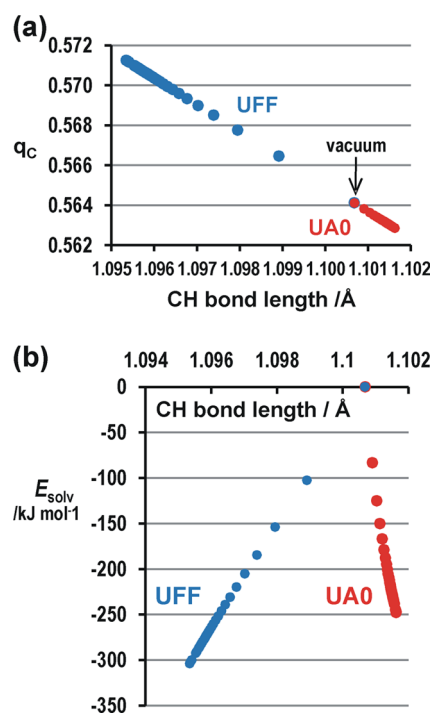


Figure 4. (a) PCM/B3LYP/aug-cc-PVDZ calculated ESP carbon atom charge q_C as a function of the optimized methyl cation CH bond length for both UA0 and UFF cavity models. (b) Corresponding solvation energies with respect to the methyl cation in vacuum.

atoms approach too close to the boundary surface prescribed by the default radius of the CH_3 united atom. In contrast, the UFF radius for H moves with the atom as the CH bond is extended.

Inspection of Figure 5 shows that the default UA0 radius for the CH_3 group (2.525 \AA) encompasses all four atoms of the

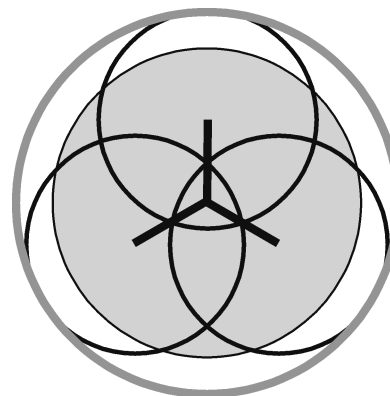


Figure 5. Atom radii for methyl cation solute cavities in continuum solvent: the outermost gray-lined circle represents the default CH_3 group radius (2.525 \AA) in the united atom topological model UA0; the innermost gray-shaded circle is the default C atom radius (2.04 \AA), and the three black-lined circles show the default H atom radius (1.44 \AA) for the united force field model UFF.

methyl cation, assuming a CH bond length of 1.1 \AA and the default UFF radii for C (2.04 \AA) and H (1.44 \AA). As the UA0 radius increases, the D_3 EIE for transfer of a methyl cation from vacuum to continuum “water” ($\epsilon = 80$) becomes less normal and tends toward unity, as shown by the AM1 results presented in Figure 6 (solid red circles); a larger cavity is more “vacuum-like” even within a high-dielectric continuum. For any particular

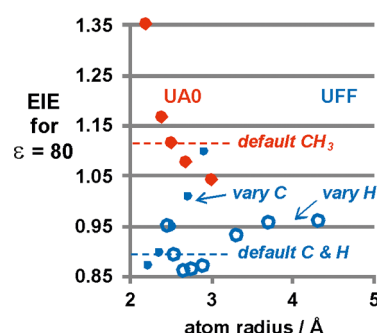


Figure 6. Calculated EIEs $K(\text{CH}_3)/K(\text{CD}_3)$ at 298 K for transfer of a methyl cation from vacuum to continuum solvent ($\epsilon = 80$) using the PCM/AM1 method, with either the UA0 (red) or UFF (blue) cavities, as a function of atom radius. Solid blue dots denote variation in the UFF C radius for constant H radius = 1.44 Å; open blue circles denote variation in the UFF H radius for constant C radius = 2.04 Å.

UA0 radius, extending the CH bond length of the methyl group within the cavity brings the H atom charge closer to the cavity boundary, where it experiences a greater degree of stabilization from the continuum dielectric; the H atom charge increases as the C atom charge decreases (Figure 4a) and the solvation energy becomes more negative (Figure 4b).

Increasing the C atom radius for the UFF cavity while keeping the H atom radius fixed at its default value causes the EIE to become less inverse and then more normal (Figure 6, solid blue dots). It might be imagined that when the UFF C atom radius is sufficiently large that it encompasses all of the H atoms, the model would behave as UA0; in the limit of a very large cavity, this must be true, but it is not so up to a value of 3 Å considered here. Strange behavior is also manifested by keeping the UFF C atom radius fixed while varying the H atom radius; the open blue circles on Figure 6 show the EIE plotted against the sum of the H atom radius plus the CH bond length (taken as 1.1 Å), which represent the longest distance from the C atom of any point on the H atom part of the cavity surface. For values of the H atom radius less than about 1.55 Å (i.e., <2.65 Å on the “atom radius” axis of Figure 6), the methyl cation UFF cavity surface has areas of both H and C atoms exposed to the dielectric continuum; for H atom radii greater than about 2.32 Å (i.e., <3.42 Å on the atom radius axis of Figure 6), the methyl cation UFF cavity surface has only H atoms exposed, and in the intermediate range, the dielectric continuum “sees” only the H atom surface in the trigonal plane but both H and C atom surfaces in the perpendicular direction. As the H atom radius increases from the smallest values, the EIE at first becomes more inverse, reaching an extremum at about 1.55 Å (2.65 Å on the graph) and then becoming less inverse and tending toward unity. It seems that exposure of the C atom surface to the continuum dielectric is responsible for the inverse EIEs. At the default values for both the C atom and H atom radii, diminishing the CH bond length from its vacuum value for the methyl cation leads to an increase in the C atom charge (Figure 4a), which is stabilized by exposure to the dielectric continuum (Figure 4b).

At this point, it is worth re-emphasizing why the CH bond length and stretching force constant respond so differently to the dielectric medium according to the UA0 and UFF cavity models with their default atomic radii. Extending the CH bond within the UA0 cavity brings the H atom charge closer to the cavity boundary, where it experiences a greater degree of stabilization from the continuum dielectric; the H atom charge

increases, the solvation energy becomes more stabilizing, and the stretching force constant is reduced. However, extending the CH bond within the UFF cavity increases the surface area of the H atom at the expense of the C atom and therefore diminishes exposure of the C atom charge to the dielectric, which results in decreased stabilization and therefore to an increased stretching force constant. The same type of behavior would be displayed for other choices of atomic radii and other varieties of solvation model; the key factor is the shape of the solute cavity, either spherical or “CPK-model”-like. For example, the same B3LYP/aug-cc-PVDZ method used with the SMD solvation model in Gaussian09 gives $K(\text{CH}_3)/K(\text{CD}_3) = 0.90$ for transfer of the methyl cation from vacuum to water, in complete agreement with the UFF result.

The B3LYP/aug-cc-PVDZ potential energy profile for the methyl cation CH bond in vacuum is anharmonic, with a good fit being obtained to a quartic function in the range of bond lengths from 0.8 to 1.6 Å. Superimposition of UA0 continuum solvation that stabilizes the cation with increasing bond length causes the equilibrium bond length to increase and the second derivative at the energy minimum (i.e., the harmonic force constant) to decrease, as shown by Halevi.³⁴ Conversely, superimposition of UFF continuum solvation that stabilizes the cation with decreasing bond length causes the equilibrium bond length to decrease and the harmonic force constant to increase. Thus, UA0 cavities lead to normal EIEs but UFF cavities lead to inverse EIEs in the PCM method.

For most purposes, it is not necessary to employ an anharmonic treatment of the vibrational frequencies, even though finite displacements in the CH bonds are best described by an anharmonic potential. This is because the average error in scaled anharmonic frequencies calculated with electronic structure methods, such as that used in this work, is very similar to that in scaled harmonic frequencies from the same method; the scaling factors have different values, but the end result is effectively the same.³⁵

CONCLUSIONS

B3LYP/aug-cc-PVDZ and AM1 calculations of secondary $\alpha\text{-D}_3$ EIEs for transfer of the methyl cation from vacuum to implicit solvent give opposite trends for UA0 and UFF cavities with the PCM method. As the dielectric constant $\epsilon \rightarrow \infty$ with the DFT method, UA0 predicts increasingly normal EIEs, tending toward ~ 1.06 , implying that the methyl cation is looser in the dielectric continuum than that in vacuum, whereas UFF predicts increasingly inverse EIEs, tending toward ~ 0.90 , implying that the methyl cation is tighter in the dielectric continuum than that in vacuum. Explicit solvent calculations using a hybrid AM1/TIP3P potential predict an $\text{EIE} = 0.85 \pm 0.02$ (at 298 K) for transfer of a methyl cation from vacuum to water, averaged over 40 different solvent configurations, in qualitative accord with the UFF result but not with UA0.

The opposing trends found with UA0 and UFF may be satisfactorily explained in terms of the different degrees of exposure of the atomic charges to the dielectric continuum in cavities of different shapes. These results are likely to be valid for other choices of atomic radii or the continuum solvent method because they depend on the shape of the solute and whether or not hydrogen atoms are included explicitly. It is reassuring to note that the UFF cavity shape is now the default model in Gaussian09.

Most of the variation in the EIE values occurs within the same range of dielectric constants as is considered to occur

within proteins and enzyme active sites. This has possible implications for computational modeling of isotope effects in enzyme-catalyzed group-transfer reactions. It is conceivable that a reaction involving charge redistribution, separation, or neutralization within an enzyme active site could manifest variations in KIEs, as between a wild-type and a mutant form of the enzyme, that originate from changes in the local dielectric response within the inhomogeneous protein environment; if so, there would be important implications for the interpretation of experimental KIEs in mechanistic enzymology.

■ ASSOCIATED CONTENT

■ Supporting Information

Vibrational frequencies, isotopic partition function ratios and EIEs for the UA0 and UFF cavities, and complete refs 25 and 26. This material is available free of charge via the Internet at <http://pubs.acs.org>.

■ AUTHOR INFORMATION

Corresponding Author

*E-mail i.h.williams@bath.ac.uk. Phone: +44 1225 386625. Fax +44 1225 386231.

Notes

The authors declare no competing financial interest.

■ ACKNOWLEDGMENTS

I.H.W. thanks Professor Iñaki Tuñón (Valencia) for helpful discussions at the Isotopes 2007 Conference in Benicassim.

■ REFERENCES

- (1) *Isotope Effects in Chemistry and Biology*; Kohen, A., Limbach, H.-H., Eds.; Taylor and Francis: New York, 2006.
- (2) Reichardt, C. *Solvents and Solvent Effects in Organic Chemistry*, 3rd ed.; Wiley-VCH: Weinheim, Germany, 2003.
- (3) Westaway, K. C. Using Kinetic Isotope Effects to Determine the Structure of the Transition States of S_N2 Reactions. *Adv. Phys. Org. Chem.* **2006**, *41*, 217–273.
- (4) Szyllabel-Godala, A.; Madhavan, S.; Rudziński, J.; O'Leary, M. H.; Paneth, P. Nitrogen and Deuterium Kinetic Isotope Effects on the Menshutkin Reaction. *J. Phys. Org. Chem.* **1996**, *9*, 35–40.
- (5) Owczarek, E.; Kwiatkowski, W.; Lemieszewski, M.; Mazur, A.; Rostkowski, M.; Paneth, P. Calculations of Substituent and Solvent Effects on the Kinetic Isotope Effects of Menshutkin Reactions. *J. Org. Chem.* **2003**, *68*, 8232–8235.
- (6) Yamataka, H.; Tamura, S.; Hanafusa, T.; Ando, T. Kinetic Isotope Effect Study of the Borderline Solvolysis of Isopropyl 6-Naphthalenesulfonate. *J. Am. Chem. Soc.* **1985**, *107*, 5429–5434.
- (7) Shiner, V. J. Deuterium Isotope Effects in Solvolytic Substitution. In *Isotope Effects in Chemical Reactions*; Collins, C. J., Bowman, N. S., Eds.; Van Nostrand Reinhold: New York, 1970.
- (8) Shiner, V. J.; Nollen, D. A.; Humski, K. Multi-Parameter Optimization Procedure for the Analysis of Reaction Mechanistic Schemes. Solvolyses of Cyclopentyl *p*-Bromobenzenesulfonate. *J. Org. Chem.* **1979**, *44*, 2108–2115.
- (9) Bentley, T. W. Secondary α -Deuterium Kinetic Isotope Effects: Assumptions Simplifying Interpretations of Mechanisms of Solvolyses of Secondary Alkyl Sulfonates. *J. Org. Chem.* **2004**, *69*, 1756–1759.
- (10) Keller, J. H.; Yankwich, P. E. Medium Effects on Heavy-Atom Kinetic Isotope-Effects. 1. Cell Model Without Internal–External Coordinate Interaction. *J. Am. Chem. Soc.* **1973**, *95*, 4811–4815.
- (11) Keller, J. H.; Yankwich, P. E. Medium Effects on Heavy-Atom Kinetic Isotope-Effects. 2. Cell Model With External–External and Certain External–Internal Coordinate Interactions. *J. Am. Chem. Soc.* **1973**, *95*, 7968–7972.
- (12) Keller, J. H.; Yankwich, P. E. Medium Effects on Heavy-Atom Kinetic Isotope-Effects. 3. Structured Medium Model Applied to Complex-Formation via Mass Point Attachment and Coupling. *J. Am. Chem. Soc.* **1974**, *96*, 2303–2314.
- (13) McKenna, J.; Sims, L. B.; Williams, I. H. Calculation of Kinetic Isotope Effects for S_N2 Bromine Exchange Reactions: Development of Transition-State Force Field for Calculation of NPE Effects. *J. Am. Chem. Soc.* **1981**, *103*, 268–272.
- (14) Williams, I. H. Theoretical Studies of Isotope Effects Pertinent to Solvolysis Mechanisms. *J. Chem. Soc., Chem. Commun.* **1985**, 510–511.
- (15) Barnes, J. A.; Williams, I. H. Theoretical Investigation of the Origin of Secondary α -Deuterium Kinetic Isotope Effects. *J. Chem. Soc., Chem. Commun.* **1993**, 1286–1287.
- (16) Ruggiero, G. D.; Williams, I. H. Computational Investigation of the Effect of α -Alkylation on S_N2 Reactivity: Acid-Catalyzed Hydrolysis of Alcohols. *J. Chem. Soc., Perkin Trans. 2* **2001**, 448–458.
- (17) Ruggiero, G. D.; Williams, I. H. Kinetic Isotope Effects for Gas Phase S_N2 Methyl Transfer: A Computational Study of Anionic and Cationic Identity Reactions. *J. Chem. Soc., Perkin Trans. 2* **2002**, 591–597.
- (18) Williams, I. H. Kinetic Isotope Effects from QM/MM Subset Hessians: “Cut-Off” Analysis for S_N2 Methyl Transfer in Solution. *J. Chem. Theory Comput.* **2012**, *8*, 542–553.
- (19) Ruiz-Pernía, J. J.; Williams, I. H. Ensemble-Averaged QM/MM Kinetic Isotope Effects for the S_N2 Reaction of Cyanide Anion with Chloroethane in DMSO Solution. *Chem.—Eur. J.* **2012**, *18*, 9405–9414.
- (20) Ruiz-Pernía, J. J.; Ruggiero, G. D.; Williams, I. H. QM/MM Kinetic Isotope Effects for Chloromethane Hydrolysis in Water. *J. Phys. Org. Chem.* **2013**, *26*, 1058–1065.
- (21) Williams, I. H. Theoretical Modelling of Compression Effects in Enzymic Methyl Transfer. *J. Am. Chem. Soc.* **1984**, *106*, 7206–7212.
- (22) Moliner, V.; Williams, I. H. Influence of Compression upon Kinetic Isotope Effects for S_N2 Methyl Transfer: A Computational Reappraisal. *J. Am. Chem. Soc.* **2000**, *122*, 10895–10902.
- (23) Ruggiero, G. D.; Williams, I. H.; Roca, M.; Moliner, V.; Tuñón, I. QM/MM Determination of Kinetic Isotope Effects for COMT-Catalysed Methyl Transfer Does Not Support Compression Hypothesis. *J. Am. Chem. Soc.* **2004**, *126*, 8634–8635.
- (24) Kanaan, N.; Ruiz-Pernía, J. J.; Williams, I. H. QM/MM Simulations for Methyl Transfer in Solution and Catalysed by COMT: Ensemble-Averaging of Kinetic Isotope Effects. *Chem. Commun.* **2008**, 6114–6116.
- (25) Frisch, M. J.; et al. *Gaussian 03*, revision B.04; Gaussian, Inc.: Pittsburgh, PA, 2004.
- (26) Frisch, M. J.; et al. *Gaussian 09*, revision A.02; Gaussian, Inc.: Wallingford, CT, 2009.
- (27) Fang, Y.; Gao, Y.; Ryberg, P.; Eriksson, J.; Kolodziejska-Huben, M.; Dybala-Defratyka, A.; Madhavan, S.; Danielsson, R.; Paneth, P.; Matsson, O.; Westaway, K. C. Experimental and Theoretical Multiple Kinetic Isotope Effects for an S_N2 Reaction. An Attempt to Determine Transition-State Structure and the Ability of Theoretical Methods to Predict Experimental Kinetic Isotope Effects. *Chem.—Eur. J.* **2003**, *9*, 2696–2709.
- (28) Williams, I. H. Force-Constant Computations in Cartesian Coordinates. Elimination of Translational and Rotational Contributions. *J. Mol. Struct.: THEOCHEM* **1983**, *94*, 275–284.
- (29) Williams, I. H. Deuterium Fractionation Factors for Carbon–Hydrogen Bonds: Calculations Using Scaled Quantum-Mechanical Force Constants. *J. Phys. Org. Chem.* **1990**, *3*, 181–190.
- (30) Field, M. J.; Albe, M.; Bret, C.; Proust-De Martin, F.; Thomas, A. The Dynamo Library for Molecular Simulations Using Hybrid Quantum Mechanical and Molecular Mechanical Potentials. *J. Comput. Chem.* **2000**, *21*, 1088–1100.
- (31) Amado, A. M.; Fiuza, S. M.; Batista de Carvalho, L. A. E.; Ribeiro-Claro, P. J. A. On the Effects of Changing Gaussian Program Version and SCRF Defining Parameters: Isopropylamine as a Case Study. *Bull. Chem. Soc. Jpn.* **2012**, *85*, 962–975.

- (32) Born, M. Volumen und Hydratationswärme der Ionen. *Z. Phys.* **1920**, *1*, 45–48.
- (33) Patargias, G. N.; Harris, S. A.; Harding, J. H. A Demonstration of the Inhomogeneity of the Local Dielectric Response of Proteins by Molecular Dynamics Simulations. *J. Chem. Phys.* **2010**, *132*, 235103.
- (34) Halevi, E. A. The Role of Electrostatic Induction in Secondary Isotope Effects on Acidity: Theory and Computational Confirmation. *New J. Chem.* **2014**, *38*, 3840–3852.
- (35) Jacobsen, R. L.; Johnson, R. D.; Irikura, K. K.; Kacker, R. N. Anharmonic Vibrational Frequency Calculations Are Not Worthwhile for Small Basis Sets. *J. Chem. Theory Comput.* **2013**, *9*, 951–954.